Thermal evaluation of zone-melting recrystallization of thin-film structures over a wide range of melting points

Richard D. Robinson, Peter Y. Wong, and Ioannis N. Miaoulis[a)]
Mechanical Engineering Department, Thermal Analysis of Materials Processing Laboratory, Tufts University, Medford, Massachusetts 02155

(Received 22 February 1994; accepted 6 December 1994)

Zone-melting recrystallization (ZMR) is a lateral epitaxy technique used to recrystallize polycrystalline thin films on substrates. Large-area multilayer structures of thin films processed with ZMR are usable in microelectronics applications. During the processing, slight variations in thermal gradients can lead to different crystalline qualities. Thus, processing uniformity over the wafer is strongly affected by the sensitivity of both the melt width and the solid/liquid interface to changes in the thermal environment. Processing control must either be set initially in a stable operating range or adjusted dynamically to variations in processing. Numerical simulations of the ZMR process were conducted to evaluate the sensitivity of the process over a wide range of temperatures and materials. Results indicate that material with melting points below 900 °C are very sensitive to temperature disturbances. This is due to the increased influence of conductive heating and decreased influence of radiative heating. The increased reflectivity during phase change curbs the amount of absorbed radiation. As the absorbed radiation becomes less influential, the sensitivity of the slush width decreases. Conductive effects should be considered when processing materials with melting points at or below 900 °C.

I. INTRODUCTION

Recrystallizing polycrystalline thin films in heterostructures can be accomplished through zone-melting recrystallization (ZMR). In particular, ZMR processing has been applied successfully to silicon-on-insulator (SOI) technology over the past decade.[1] Devices made from SOI material can operate at high voltages and high temperatures, and are radiation hardened. Also, microelectromechanical devices such as sensors or actuators have been developed using SOI material processed by ZMR.[1] Some of the newer ZMR technologies include the processing of multiple films undergoing recrystallization,[2] nonplanar film structures,[3,4] large areas films,[5,6] and electronic materials other than silicon.[7] The heat transfer and crystallization dynamics vary for these different technologies. Thus, to evaluate them, a fundamental understanding of the heat transfer mechanisms in the process is needed.

ZMR is a lateral liquid-phase epitaxy process used to recrystallize amorphous or polycrystalline films into a single crystal. Typically, a lower susceptor heats the film structure uniformly to a temperature near its melting point. A line heater situated above the wafer heats a narrow region, creating a molten zone in the thin film (Fig. 1). As the line heater is scanned over the film the material in the wake of the moving molten zone recrystallizes in the form of a single crystal. The narrow heat zone can be generated by several means: scanned laser beam, electron beam, incandescent lamp, or radiant graphite strip. A graphite strip with a square cross section is simulated in this investigation. In this case, the strip heater, wafer, and susceptor are enclosed in a water-cooled chamber with an argon atmosphere.

The ZMR processing of silicon wafers and silicon-on-insulator (SOI) structures has been studied by numerous investigators.[6,8–16] Their analyses revealed various physical phenomena that occur during processing. In particular, the size of the molten zone and the crystallization dynamics at the solid/liquid interface were found to be strongly affected by the difference in radiative properties between solid and liquid phases,[15,16] the radiative distribution from the line heater,[16] the lower susceptor intensity,[16] supercooling in the liquid phase,[6,17] and scan speed.[12,17] Both the critical processing parameters (e.g., heat source intensity, susceptor temperature, and reflector design) and the film structure designs (e.g., film thicknesses and seed window locations) have been optimized to accommodate the sensitive nature of the melt width and the interface morphology. As stated earlier, this has resulted in the development of a mature silicon ZMR technology. However, quite little has been done on processing materials other than silicon (T_m = 1412 °C). Recently, research on gallium films (T_m = 30 °C) for low temperature ZMR processing has been

[a)]Author to whom all correspondence should be addressed.

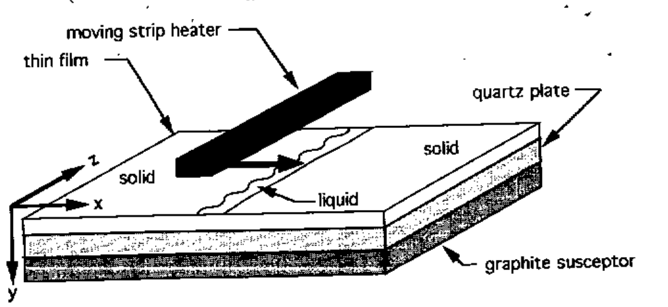

FIG. 1. Schematic of a typical ZMR processing using a line heat source.

reported[7] which revealed significant differences in the heat transfer dynamics.

Potential electronic materials that can be used in thin-film microelectronic devices exhibit a wide range of melting points. These include Ga (30 °C), Se (217 °C), Ge (937 °C), and the new III-V electronic materials InSb (535 °C), GaSb (710 °C), and InP (1070 °C). The application of modern material processing techniques, including ZMR, is dependent on the heat source characteristics and the thermophysical properties of all the materials in the film structure. In particular, the modes of heat transfer (conduction, convection, and radiation) in the processing chamber have different levels of influence depending on the melting point of the material.[18]

An extreme example of the different levels of influence can be seen by comparing silicon and gallium, Ga, ZMR processing. The strip heater temperature in silicon processing is above 2000 °C, whereas the strip heater temperature in gallium processing is around 250 °C. In gallium processing, the conductive flux from the strip heater through the gas is the dominant heating mechanism. This is in contrast to silicon processing where the radiative flux is the dominant mode of heat transfer. The conductive heat flux from the strip heater to the wafer travels through a stagnant region of gas below the strip heater.[7,19] In silicon ZMR, different ambient gases produce different temperature profiles in the film, even though heating is dominated by radiation.[19] Moreover, the stability of the interface and the quality of the resultant crystal are dependent on the type of heating (i.e., radiative or conductive).[7,12,15] Clearly, the heat transfer issues must be addressed in more detail in order to apply the ZMR process to materials other than silicon.

Two issues that need to be addressed for processing any material are the capability of producing low defect densities and the processing uniformity. The defect form and the defect densities are greatly affected by the solid/liquid interface morphology. This morphology may be nonplanar because of the destabilizing microscale heat transfer effects.[9,12,15,17,20] Nonplanar morphologies that may develop include repeating cellular, faceted, and dendritic structures. These structures develop due to the modes of heating, thermophysical properties, crystalline structure, and impurities. Since the influence of each of these phenomena can vary greatly between materials and melting points, certain materials may have combined effects that prevent acceptable defect densities from developing.

Provided that a suitable interface morphology can be generated, the second issue to consider is the continual propagating of the interface over the wafer. In silicon ZMR processing, processing uniformity has been found to vary over the wafer.[3,4] Processing uniformity is affected by the sensitivity of the interface to perturbations from either the heating environment or the film structure. Thus, processing parameters must be set to conditions where the molten zone is the least sensitive to perturbations in order to ensure continual propagation of the interface. Dynamic control of the process can solve some of the problems. But certain materials are always highly sensitive to perturbations and, consequently, may not be suitable for ZMR. Thus, to evaluate the feasibility of using the ZMR process for a specific material, one must determine the significant heat transfer modes for the given melting point, the capability to develop an adequate interface morphology, and the sensitivity of the melt region to perturbations.

This paper presents the results of a numerical investigation of the heat transfer effects in ZMR processing of materials with melting points that span a wide range of temperatures. Numerical models are used to calculate the heat transfer and fluid flow in the processing chamber, as well as the heat transfer and melting in the film. These models are described in the next section. The range of solid/liquid interface morphologies that can develop are described, along with the microscale heat transfer effects which produce them. Also, the stability of the molten zone is found through parametric studies. The phenomena responsible for the sensitivity of the molten zone to parameter changes are analyzed as well. In the past, investigative studies on ZMR processing have been solely limited to the recrystallization of silicon. This analysis provides insight into the heat transfer dynamics and processing uniformity for materials other than silicon.

II. MODELING

The ZMR process can be examined in two parts: the heat transfer in the chamber (external parameters) and the heat transfer in the wafer (internal parameters). The physical and numerical models are discussed relative to these two parametric sets.

A. Physical model

For these studies, the external parameters include the lower susceptor, the line heater, and the chamber walls.

The specific dimensions of these parameters were chosen to reflect as typical ZMR setup, but results are generally applicable to other setups. The size of the chamber is considered to be 10 cm wide and long, and 6 cm tall. The ambient gas in the chamber is argon at atmospheric pressure. The walls of the chamber are considered to be water cooled to a temperature of 30 °C. The film structure rests on a quartz sheet, which is 3 mm thick. The quartz sheet rests atop the lower susceptor heater, which is typically a flat graphite sheet. Thus, heat from the susceptor arrives to the film in two ways; radiative heating passing through the semitransparent quartz sheet and conductive heating through the quartz sheet.

The line heater is a resistively heated graphite strip with a square cross section of 3 × 3 mm. The spacing between the strip heater and the film is 1.5 mm. In the space between the heater and the film, a stagnant region of gas forms which allows heat to travel conductively between the two surfaces. Beyond the stagnant region, there is convective cooling of the film. The strip heater is a radiative black body with a constant temperature surface. Radiation from the graphite strip heater is distributed over the film with a distinct profile depending on the size and geometry of the heater.[9]

The internal parameters of the film structure include the properties of the substrate and the recrystallizing thin film. In these studies, the substrate is always made of crystalline silicon. The dimensions of the substrate are 60.0 mm wide and long, and 0.5 mm thick. The substrate is considered to not melt or warp during processing. The thermophysical properties of the substrate are considered to be constant.[9]

A discrete range of different thin film materials is examined. Each thin film is characterized primarily by its melting point. Thermophysical and radiative properties of both liquid and solid phases for most of the new III-V materials are lacking in literature; consequently, the properties of silicon are used as a base with which to work. The reflectivity of the solid phase of the material is assumed to always be 0.3, while the liquid phase reflectivity is 0.7. The emissivity of the material is 0.7 in solid phase and 0.3 in liquid phase. This represents the typical behavior of electronic materials which become more metallic upon melting. Thermal conductivity in the solid phase is 0.3 W/cm °C and 0.7 in the liquid phase. The density of the material is 2.33 g/cm^3 and the specific heat is 0.927 J/g °C.

B. Numerical model

The strip heater temperature, heat flux over the film, and the temperature distributions in the film are solved through an iterative procedure[19] using two numerical models. One model determines the heat transfer and fluid flow in the chamber, the other determines the heat transfer dynamics and melting in the film.

The argon gas flow in the chamber is determined using FLOTHERM™ software.[21] The water-cooled wall temperature is fixed at 30 °C. For these studies, the strip heater is considered to be stationary above the center of the film. This has been found to be a good approximation for high temperature processing[22] and low scan speeds (<300 μm/s).[17] However, at low processing temperatures, there is a significant difference between stationary and moving results.[7] Stationary conditions are studied here to provide baseline results for all processing temperatures. The temperature distribution in the film is set to resemble actual ZMR conditions, with the center at the melting point and edges at the susceptor temperature. The uniform susceptor temperature is set to 95% of the melting point of the thin film material. The strip heater temperature is also considered uniform and constant. As the strip heater temperature is changed, the conductive heat flux to the wafer changes. These changes are input into the film model The correct value of the strip heater temperature is determined iteratively between the chamber model and the film model.

The film is modeled with a transient two-dimensional control-volume formulation of the enthalpy approach. The temperature of the control volume is held at the melting temperature until the enthalpy of the control volume surpasses the latent heat of fusion (100 J/g). Thereafter, the temperature is allowed to increase normally. The change in properties with melting is modeled as changing linearly with the solid/liquid fraction. This allows for a smooth transition in modeling melting. Details of the model are given elsewhere.[9,23]

Often, the calculated incomplete melting of a region can be interpreted as a nonplanar interface. This partially melted region, where the control volume has a solid/liquid fraction between 0 and 1, is known as the "slush" region. Physically, large slush widths are associated with dendritic solidification having numerous grain boundaries. Smaller slush widths may represent a cellular interface morphology which has low defect densities. Planar interfaces, when the slush width is zero, typically have branching dislocations. Numerous factors, including the internal and external parameters, determine the size of the slush and complete liquid regions. The stability of these regions can be examined using the model. Explosive melting conditions and radiatively stable cases have been found in high temperature processing with silicon film structures.[16] In low temperature processing of gallium, slush regions cannot be created unless motion is considered in modeling.

III. RESULTS

Parametric studies of ZMR processing materials with different melting points were conducted to determine the magnitude of the heating modes, the range of slush widths, and the sensitivity of the slush widths to perturbations. Depending on the strip temperature, the conductive heat flux through the gas and the radiation from the strip exhibited differing levels of influence. The region of critical importance in the ZMR process is the melting zone, and since this zone is very narrow it lies completely under the strip. Therefore, all heat flux calculations were exclusively from this region. Slush widths are determined within a tolerance of 50 μm due to the numerical grid size. The sensitivity of the slush widths to perturbations was tested by varying the strip heater temperature. The strip heater temperature was varied over a range where slush width increased from zero to a maximum value.

A. Minimal ZMR conditions

In ZMR, certain minimal conditions must be established before processing. As the solid material is heated, it first becomes a slush, in which the material is partially molten and at the melting point temperature. Subsequently, the melting becomes "fully developed" with a centrally located liquidus region where the temperature is above the melting point, flanked by two slush regions where the material is at the melting point. One of the "minimal ZMR conditions" for successful processing is a fully developed molten zone. The forward slush region (in the direction of scanning) of a developed molten zone is the melting front. The trailing edge is the solidification front. The solidification slush region is of primary concern since it critically affects the crystalline quality.

Stable slush regions are caused by the difference in radiative properties between the solid and liquid phase, which creates a heat balance. This has been clearly demonstrated in silicon ZMR processing.[16,24] When a material's reflectivity increases upon melting (as it does for silicon and other similarly used electronic materials), the higher levels of reflectivity reduce the amount of incident radiation that is absorbed. With the reduction in radiative heat, the portions of the material at the melting temperature lack sufficient energy to undergo the complete transition from solid to liquid, and remain as a slush. More specifically, the "reflectivity heat balance" prevents the enthalpy of the material in this region from reaching the latent heat of fusion. Thus, when a molten zone is formed it acts to cut back the influence of the radiative heating. Changes in emissivity also affect the growth of the molten zone. When emissivity decreases upon melting (again, as it does for silicon and other electronic materials), there is a reduction of emissive cooling, leading to higher film temperatures and larger melt widths. So the reflectivity and emissivity effects tend to counter each other. However, thermal conditions control their relative influence: when the susceptor temperature is not exceedingly high, the reflectivity effect dominates and leads to better quality crystals.[6,11,13]

Unlike the radiative heating, the conductive heating component is not affected by the material's phase change. The thermal conductivity of the material in either the solid or liquid phase is much greater than the thermal conductivity of the ambient gas. Thus, the gas property is the limiting factor in conductive heat transfer between the strip heater and the film. When the thermal conductivity of the thin film changes, the overall thermal resistance does not change significantly. This means that the incident conductive heat flux is never subject to a cutback in power.

Earlier studies have focused on the conditions required to reach the "breakthrough point."[18] The breakthrough point is marked by the first occurrence of melting. A small increase in strip temperature is required to create minimal ZMR conditions from the breakthrough point. During the transition from the breakthrough point to minimal ZMR conditions, the effects of the reflectivity heat balance begin to appear. Figure 2 shows the effects of the reflectivity heat balance as a molten zone forms, for a material with a melting point of 500 °C. As the strip temperature increased from the breakthrough point to minimal ZMR conditions, the percentage of incident energy that is absorbed decreased from 74% to 59%. This is due to the creation of the highly reflective molten zone, which reduced the amount of absorbed radiation.

Within the slush width is the solid/liquid interface. The morphology of this interface is an important consideration in ZMR processing. The solidification front considerably influences the crystalline quality in ZMR

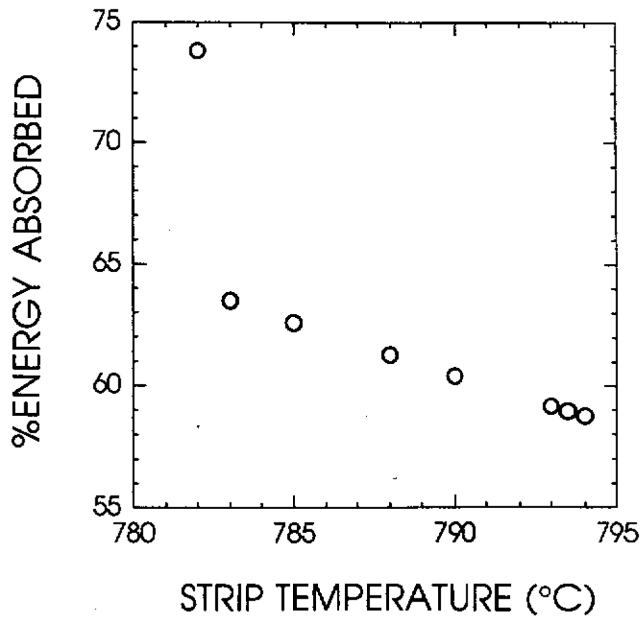

FIG. 2. Percentage of total energy absorbed as a function of strip temperature, between breakthrough point and minimal ZMR conditions. The melting point was 500 °C.

processed materials. The solidification interface morphology is an indicator of various material defects. Often this morphology is nonplanar due to the destabilizing microscale heat transfer effects (see Sec. I). The most common imperfection found in materials processed by ZMR is low-angle sub-grain boundaries, or sub-boundaries. Sub-boundaries are defined as defects that have a crystallographic angular misalignment on the order of 1° from the growth axis. It is commonly understood that defect trails and sub-boundaries form at the interior corners of faceted salification interfaces and at the re-entrant cusps of cellular solidification interfaces. Im *et al.*[12] found that a stable cellular morphology produced the highest quality silicon crystals. Both Im[24] and Grigoropoulos *et al.*[25,26] concluded that the reflectivity heat balance was the driving force behind the cellular interface in silicon.

At melting points lower than that of silicon, however, the conductive heat flux from the strip plays a larger role in the heating. And unlike the radiative heating that becomes checked by the increased reflectivity of the material upon melting, the conductive heat flux is never subject to a cutback in power. Thus, the reflectivity heat balance, and its control over the melting dynamics, is less influential at lower melting points. This can destabilize the slush regions where the cellular structures are thought to exist. However, additional thermophysical factors can create and stabilize the cellular structures, and thus the slush regions. Impurities, for instance, can perturb the solidification interface, creating regions where solid and liquid coexist. When a crystal grows from solution it usually rejects impurities (either the solute or solvent).[27] If the impurities concentrate at the crystallizing front faster than diffusion can transport them, the liquidus temperature becomes depressed.[27–29] Constitutional supercooling occurs when the temperature of the liquid in front of the interface is below the equilibrium liquidus temperature.[30] The supercooling causes an instability in the planar solidification interface because any protrusion of solid into the supercooled liquid region would not disappear.[31] The protrusions become regular features on the solidification interface, forming cellular structures. Constitutional supercooling effects in high temperature silicon ZMR have a very small effect on processing,[6] but may play a larger role at lower temperatures.[7]

B. Modes of heat transfer

In this study, the amounts of radiation and conduction absorbed by the film from the strip heater were determined for six melting points: 30 °C, 200 °C, 500 °C, 700 °C, 1000 °C, and 1400 °C. These correspond roughly to the melting point of gallium (Ga), selenium (Se), indium-antimony (InSb), gallium-antimony (GaSb), indium-phosphide (InP), and silicon (Si), respectively. The strip heater temperature was varied over the range where minimal ZMR conditions existed (i.e., while stable slush zones were present). Results from earlier studies at the breakthrough point determined that for melting temperatures below 800 °C, conduction provided up to 15% of the heating.[18] Clearly, radiation is a dominant mode of heat transfer for materials with melting points above 800 °C. For these materials, processing results similar to silicon are expected. However, processing uniformity can still be largely affected by the conductive heating component for all melting points.

Figure 3 shows the ratio of incident conductive to incident radiative heating, η_i, for different melting points. At each melting point, the full range of strip temperatures that create minimal ZMR conditions was considered—from the onset of minimal ZMR conditions to their cessation at higher strip temperatures. But the variance in η_i values through this range was so slight that it does not appear in Fig. 3. At a melting point of 700 °C, for instance, the value of η_i at the onset of ZMR conditions was 0.0897. At the cessation of ZMR conditions, η_i was 0.0898. This means that the percentage of conductive to radiative incident heating is constant and predictable for each melting point. For example, at 700 °C one can expect conductive incident heating to be always about 9% of the radiative incident heating.

As the melting point is increased, η_i dropped sharply. To illustrate, at a melting point of 500 °C, the average η_i value was 0.143. But at a melting point of 1412 °C, the average η_i value was only 0.024. The rapid decline in η_i is due to the nonlinear nature of

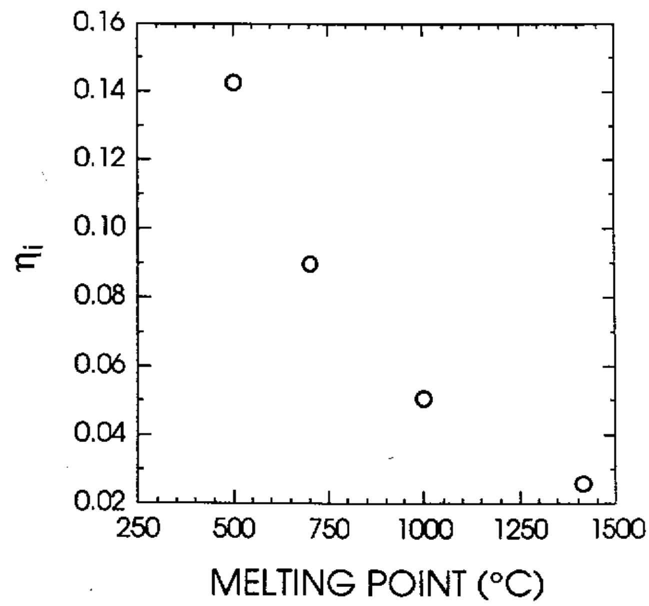

FIG. 3. Ratio of incident conductive to incident radiative heating, η_i, plotted as a function of melting point, over the range of minimal ZMR conditions.

radiative heating. As temperature increases, radiative heating increases quadratically, but conductive heating increases only linearly. This accounts for the parabolic relationship between melting point and η_i, seen in Fig. 3. In thermophysical terms, the rapid decline indicates that conductive effects become much more influential to the processing as the melting point decreases. Radiation, however, remains the dominant form of incident heating for all melting points above 500 °C, where the value of η_i was always below 0.15.

It should be noted that the two lowest melting points, 30 °C and 200 °C, do not appear on the figure. This is because slush regions proved to be unstable for these melting points. Without stable slush regions, minimal ZMR conditions cannot be satisfied. We wish to stress, however, that these results are from specific thermal conditions and do not entirely preclude the existence of slush for these two melting points. Other thermal conditions exist that allow stable slush regions for these melting points.[7]

In the same study, the modes of heat transfer within the film were examined by analyzing the ratio of absorbed conductive to absorbed radiative heating, η_a. The full range of strip temperature that create minimal ZMR conditions was considered. The relationship between η_a and the melting point (Fig. 4) is similar to that of η_i; as the melting point increased, η_a decreased parabolically. The η_a values, however, were higher than the η_i values at the same melting points. The reason for this is the reflectivity heat balance, caused by an increase in the material's reflectivity upon melting (see Sec. III. A). The increased reflectivity reduces the amount of absorbed radiative heat, but does not affect the conductive heat, so the ratio η_a increases. Since the melt zone width becomes large before minimal ZMR conditions cease to exist, the amount of absorbed radiative heat is substantially decreased. This effect substantially increases η_a at the upper limits of minimal ZMR conditions (see Fig. 4). For example, at a melting point of 1000 °C, η_a increased from 0.0913 at the establishment of minimal ZMR conditions to 0.1459 just before the stable slush regions disappear. This change in η_a is large compared to the relatively insignificant change in η_i. The large increase in η_a indicates that conductive heating becomes more influential as the molten zone grows. The increase in conductive heating influence is illustrated in Table I. The percentage of total energy absorbed that is from conductive heating increased as the melt width increased. At the melting point of 1000 °C, the percentage of total energy absorbed that is from condition increased from 8.4% at the onset of ZMR conditions to 12.7% at the cessation of ZMR conditions.

The percentage of conductive heating is significant for melting points up to about 900 °C. Above this melting point conductive heating never accounts for more than 15% of the total heat absorbed. For melting points lower than 900 °C, attention should be given to the conductive heating component. This includes the scrutiny of the ambient gas in the chamber. Previous studies indicate that the conductive heat transfer can increase by as much as six times between different gases.[19]

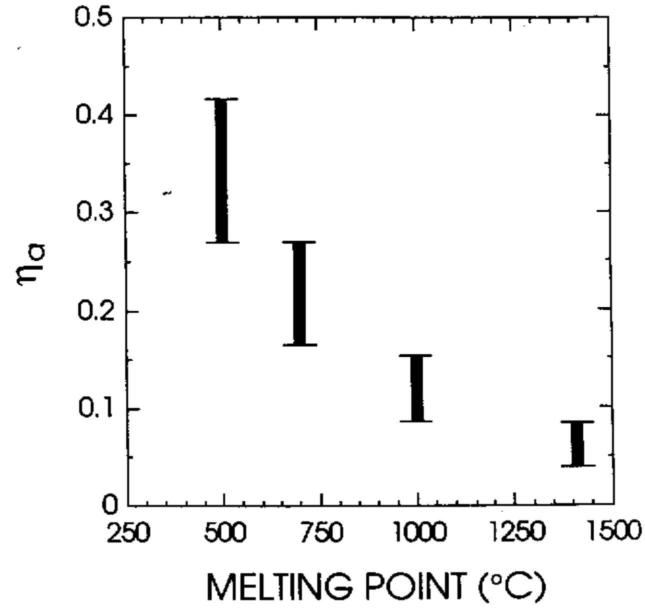

FIG. 4. Ratio of absorbed conductive to absorbed radiative heating, η_a, plotted as a function of melting point, over the range of minimal ZMR conditions.

In a broader sense, the η_a results define the processing window for ZMR. Different materials and strip heater setups will engender different profiles and modes of incident heating. But if the combination of material properties and modes of heat transfer place η_a within the ranges shown, then conditions for minimal ZMR exist. This is because η_a is a measure of the film's internal heat transfer dynamics only. Regardless of how the radiative and conductive heat are delivered to the film, if the absorbed ratio (η_a) falls within the correct bounds, then minimal ZMR conditions exist. Thus, Fig. 4 charts the processing window for ZMR.

C. Sensitivity of the slush width

Processing uniformity is related to the sensitivity of the slush width to thermal perturbations. Here, the

TABLE I. Percentage of total energy absorbed from the strip that is conductive heat, over the range of minimal ZMR conditions at each melting point.

Melting point	Percent of conductive heating
500	21.6–29.1
700	14.5–20.8
1000	8.4–12.7
1412	4.3–7.1

sensitivity is defined as the change in slush width to the change in total incident heat flux. A highly sensitive slush width indicates that the solidification-interface morphology is easily perturbed. The perturbation can vary the interfacial structure type (e.g., from cellular to dendritic) as well as amplitude and spacing of the structure. This results in spatial variations in defect type and density during processing.

The sensitivity of the slush width to changes in the total strip heat flux (radiative and conductive) is shown in Fig. 5. The increasing sensitivity for decreasing melting point (Fig. 5) is caused by the growing dominance of radiative heating. As the melting point increases, radiation becomes a more dominant form of heating. As stated earlier, radiative heating is subject to cutbacks in power from the reflectivity changes of the material. This creates a reflectivity heat balance and leads to stable slush regions (see Sec. III. A). So as radiative heating becomes dominant, the stability of the slush regions increases. The increase in stability accounts for the decreasing sensitivity of the slush regions at higher melting points. In practical terms, this indicates that materials with higher melting points are easier to process by ZMR because their processing control is easier.

During the ZMR process various thermal perturbations can create undesired fluctuations in the incident heat flux. These fluctuations lead to unpredictable and nonuniform results, reducing the processing uniformity. But the less sensitive the material is to the thermal fluctuations, the more likely processing uniformity will be maintained. The thermal perturbations come from three main sources: changes in the film's geometry,

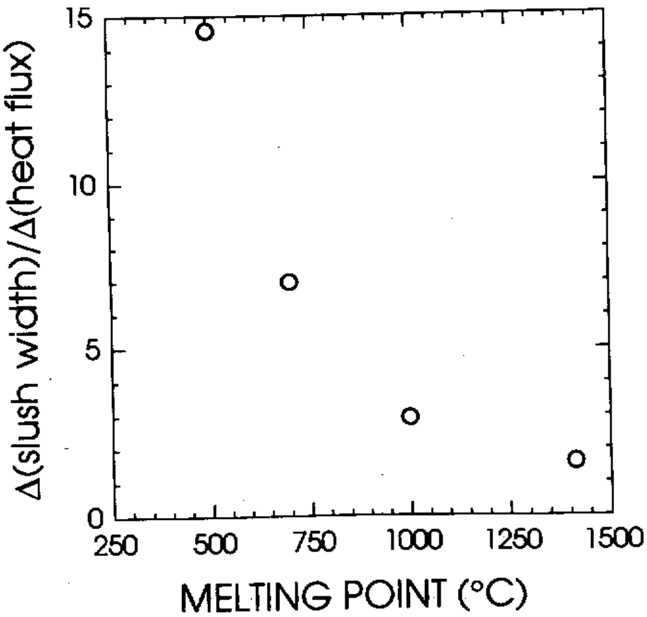

FIG. 5. Sensitivity of slush width to change in heat flux, plotted as a function of melting point.

changes in the strip heater's geometry or optical properties, and changes in the thermal environment. The geometry of the film inevitably changes for wafers that are circular. From an overhead perspective, the wafer's area widens as the strip heater approaches the wafer's center, then decreases past the center as it nears the edge. The change in wafer area changes the heat transfer dynamics within the wafer, which can cause thermal perturbations. This effect has yet to be analyzed in literature. Another film geometry concern that may trigger thermal perturbations is film thickness irregularities and stepwise structural perturbations. Examples of stepwise structural perturbations include intermittently spaced areas of pure crystal seeds and microelectronic device structures. These material variations can react with the heat transfer dynamics, disturbing the solid/liquid interface and creating material defects.[32]

The thermal perturbations from the geometry of the strip heater are due to the mechanics of graphite strip ZMR. Thermal expansion at high temperatures causes the graphite strip to sag. If the sag is not completely compensated for, heating will be nonuniform. Also, since the strip is resistively heated, the temperature distribution across it is not uniform; it is parabolically shaped with the hottest point at the lateral center (along the length of the strip). The optical properties of the strip may change if oxide or other contaminants are present on the graphite strip, in which case the radiative heat from the strip becomes nonuniform.

The thermal environment may also cause thermal perturbations. Fluctuations in the chamber or susceptor temperature can alter the conductive, radiative, and convective heat transfer of the process. Slight variations in ambient chamber gas, for example, can significantly alter the conductive heat flux from the strip heater.[19]

Even within the ZMR processing window there are conditions that are more stable than others. For example, a 100 μm slush width is the most stable slush width for a material with a melting point of 1000 °C. Figure 6 shows the solidification slush width as a function of input heat flux. The 100 μm slush width extends over the largest range of input heat flux, evidencing its stability. If the slush width is constant throughout the processing, the solidification interface cannot drastically change its morphology. This better ensures processing uniformity.

IV. CONCLUSIONS

The modes of heat transfer in ZMR processing were examined over a wide range of melting temperatures. These melting temperatures correspond to potential electronic materials, other than silicon, which can be used in thin film microelectronic devices. Both the heat transfer and melting in the film structure and the heat and fluid flow in the processing chamber were modeled numerically. As the melting point increased, the ratio of

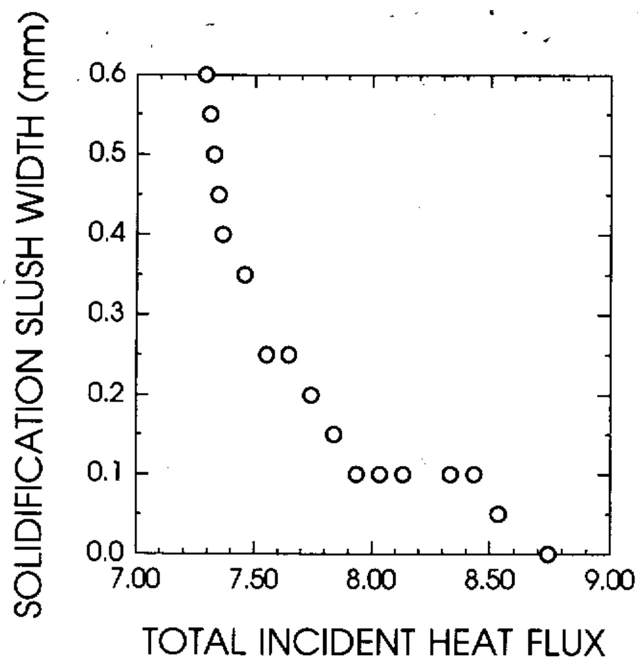

FIG. 6. Solidification slush width plotted as a function of strip temperature for a melting point of 1000 °C.

incident conductive to incident radiative heating from the strip, η_i, decreased parabolically. The same decrease was found for the ratio of absorbed conductive to absorbed radiative heating, η_a. But due to the increase in the film's reflectivity upon melting, the η_a values were higher than their η_i counterparts. The increased reflectivity curbs the amount of absorbed radiation. As the molten zone grows, this effect grows. The percentage of conductive heat absorbed can increase by as much as 9% over the range of minimal ZMR conditions at any melting point. Conductive heat transfer was found to be significant especially when considering the amount of absorbed heat. In general, conductive effects should be considered when processing materials with melting point at or below 900 °C. Processing uniformity was found to be most stable at higher melting points because of the reflectivity heat balance effects. The sensitivity of the slush width to changes in total incident heat flux decreased parabolically with melting point. Results indicated that materials with melting points below 900 °C are very sensitive to temperature disturbances.

ACKNOWLEDGMENTS

This research was supported by the National Science Foundation under Grants EID-9017557 and CTS-9157278.

REFERENCES

1. P.M. Zavracky, Solid State Technol. **34**, 55 (1991).
2. P.W. Mertens and H.E. Maes, *IEEE SOS/SOI Technology Conference* (IEEE, New York, 1990), p. 55.
3. B. Tillack, R. Banisch, H.H. Richter, K. Höppner, and O. Joachim, Mater. Sci. Eng. **B15**, 1 (1992).
4. B. Tillack, R. Banisch, F. Januschewski, H.H. Richter, K. Höppner, and A. Chovet, Mater. Sci. Eng. **B18**, 181 (1993).
5. S.M. Sze, *VLSI Technology* (McGraw-Hill, New York, 1983), p. 84.
6. P.W. Merteps, Thesis, Katholieke Universiteit Leuven, Belgium (1991) (University Microfilms Incorporated dissertation services, Ann Arbor, MI, 1992).
7. R.D. Robinson and I.N. Miaoulis, J. Appl. Phys. **75**, 1771 (1994).
8. C.K. Chen, M.W. Geis, B-Y. Tsaur, R.L. Chapman, and J.C.C. Fan, J. Electrochem. Soc. **131**, 1707 (1984).
9. I.N. Miaoulis, P.Y. Wong, J.D. Lipman, and J.S. Im, J. Appl. Phys. **69**, 7273 (1991).
10. L. Pfeiffer, A.E. Gelman, K.A. Jackson, and K.W. West, in *Beam-Solid Interactions and Transient Processes*, edited by M.O. Thompson, S.T. Pieraux, and J.S. Williams (Mater. Res. Soc. Symp. Proc. **74**, Pittsburgh, PA, 1987), p. 543.
11. R.D. Robinson and I.N. Miaoulis, J. Appl. Phys. **73**, 439 (1993).
12. J.S. I, C.K. Chen, C.V. Thompson, M.W. Geis, and H. Tomita, in *Silicon-on-Insulator and Buried Metals in Semiconductors*, edited by J.C. Sturm, C.K. Chen, L. Pfeiffer, and P.L.F. Hemment (Mater. Res. Soc. Symp. Proc. **107**, Pittsburgh, PA, 1988), p. 169.
13. D. Dutartre, Mater. Sci. Eng. **B4**, 211 (1989).
14. M.W. Geis, H.I. Smith, D.J. Silversmith, R.W. Mountain, and C.V. Thompson, J. Electrochem. Soc. **130**, 1178 (1983).
15. K.A. Jackson and D.A. Kurtze, J. Cryst. Growth **71**, 385 (1985).
16. J.S. Im, J.D. Lipman, I.N. Miaoulis, C.K. Chen, and C.V. Thompson, in *Beam-Solid Interactions: Physical Phenomena*, edited by J.A. Knapp, P. Borgesen, and R.A. Zuhr (Mater. Res. Soc. Symp. Proc. **157**, Pittsburgh, PA, 1990), p. 455.
17. S.M. Yoon and I.N. Miaoulis, J. Mater. Res. **7**, 124 (1992).
18. R.D. Robinson and I.N. Miaoulis, in *Crystallization and Related Phenomena in Amorphous Materials*, edited by M. Libera, T.E. Haynes, P. Cebe, and J.E. Dickinson, Jr. (Mater. Res. Soc. Symp. Proc. **321**, Pittsburgh, PA, 1994), p. 627.
19. B.D. Heilman, M.A. Marston, P.Y. Wong, and I.N. Miaoulis, J. Mater. Res. **8**, 551 (1993).
20. W.W. Mullins and R.F. Sekerka, J. Appl. Phys. **35**, 444 (1964).
21. *The Flotherm Reference Manual* (Flomerics Limited, England, 1992).
22. J.D. Lipman, Thesis, Tufts University, Medford, MA (1989).
23. J.D. Lipman, P.Y. Wong, I.N. Miaoulis, and J.S. Im, *HTD-Vol. 123, Collected Papers in Heat Transfer* (The American Society of Mechanical Engineers, New York, 1989), pp. 211–217.
24. J.S. Im, Ph.D. Thesis, Massachusetts Institute of Technology (1989).
25. C.P. Grigoropoulos, R.H. Buckholz, and G.A. Domoto, J. Appl. Phys. **59**, 454 (1986).
26. C.P. Grigoropoulos, R.H. Buckholz, and G.A. Domoto, J. Appl. Phys. **62**, 474 (1987).
27. B. Chalmers, *Principles of Solidification* (John Wiley and Sons, New York, 1964), pp. 143–157.
28. D.P. Woodruff, *The Solid-Liquid Interface* (Cambridge University Press, London, 1973), p. 83.
29. W.W. Mullins and R.F. Sekerka, J. Appl. Phys. **35**, 444 (1964).
30. C.A. Knight, *The Freezing of Supercooled Liquids* (D. Van Nostrand Co., Toronto, 1967), p. 87.
31. M.C. Flemings, *Solidification Processing* (McGraw-Hill, New York, 1974), p. 59.
32. C.K. Hess, P.Y. Wong, and I.N. Miaoulis, *HTD-Vol. 196, Transport Phenomena in Materials Processing and Manufacturing* (The American Society of Mechanical Engineers, New York, 1992), pp. 221–223.